LIMITS ON TURBULENT H I FLUCTUATIONS TOWARD PSR B0329+54 ON SCALES BETWEEN 0.0025 AND 12.5 AU

ANTHONY H. MINTER,[1] DANA S. BALSER,[1] AND JEYHAN S. KARTALTEPE[2,3]

ABSTRACT

We have measured the H I absorption toward pulsar B0329+54 using the Green Bank Telescope during 18 epochs between 2002 June 30 and 2003 October 10. Three observing epochs consisted of a continuous period of 20 hr each, while 15 epochs were 1–2 hr each. We calculate the structure function of H I absorption variations toward the pulsar on timescales of 10 minutes to 16 months, which using the proper motion of 95 km s^{-1} and the parallactic distance of 1.03 kpc measured toward B0329+54 (Brisken et al.), corresponds to angular scales of 0.37 μas to 23.8 mas and samples structures between 0.0025 and 12.5 AU, assuming H I gas halfway to the pulsar and ignoring scintillation effects. We find no evidence for any turbulent H I absorption fluctuations toward B0329+54, with the following upper limits on $\Delta\tau$ for various absorption features: 0.026 at −31, −21, −18, and +4 km s^{-1}; 0.12 at −11 km s^{-1}; and 0.055 at −1 km s^{-1}.

Subject headings: ISM: clouds — ISM: structure — pulsars: individual (B0329+54) — radio lines: ISM — turbulence

1. INTRODUCTION

During the last decade, studies of H I absorption lines have revealed angular or temporal variations corresponding to spatial scales on the order of tens of AU. In some directions structure in the H I has been observed and interpreted as individual H I clouds passing across the line of sight with densities of 10^4–10^5 cm^{-3}. Based on these measurements, a significant fraction (10%–15%) of the cold H I gas must be in these clouds (Frail et al. 1994). However, it is difficult to reconcile the high H I densities at AU scales implied by these measurements with other information about the interstellar medium (ISM), as they would be greatly out of pressure equilibrium and should be short lived. Heiles (1997) proposed that the observed H I components are formed from sheets and filaments where the large column densities are produced by the appropriate viewing angle. Deshpande (2000) suggests that these data have been misinterpreted and that a single power law describes the distribution of cold H I in the ISM. It has also been suggested that the observed changes in the H I absorption profiles toward pulsars are the result of scintillation along with a velocity gradient in a uniform H I medium (Gwinn 2001). Angular power spectra from H I emission observations reveal a power-law distribution of H I structures on parsec scales consistent with a turbulent medium (e.g., Green 1993). It seems possible that the AU-scale H I fluctuations are part of the same turbulence that is present on parsec scales, but this has not been conclusively demonstrated.

If AU-scale fluctuations are present and are part of the turbulent cascade seen at parsec scales, then it may be possible to determine some of the fundamental characteristics of the H I gas. If the gas is purely hydrodynamic (HD), then the smallest size scale that shows fluctuations, called the inner scale, is larger than the "molecular" mean free path length (Tennekes &

Lumley 1994; Frisch 1995). For typical situations in the ISM the H I mean free path length corresponds to scales from ∼1 to 100 AU. Collisions of the H I with the ions and electrons in magnetohydrodynamic (MHD) turbulence could create H I fluctuations on scales smaller than ∼AU. If we are able to measure the inner scale of the HD turbulence, then it is possible to estimate the kinematic viscosity of the H I in the ISM. The kinematic viscosity is given approximately by $\nu \sim \lambda_{\mathrm{mfp}} c_{\mathrm{th}}$, where λ_{mfp} is the mean free path length and c_{th} is the thermal sound speed. If the H I turbulence is MHD, then sub-AU scale H I fluctuations would be present, which would tell us that magnetic fields cannot be ignored in any aspect of the dynamics of interstellar gas.

We have made H I absorption measurements toward the pulsar B0329+54 with the Green Bank Telescope (GBT) to measure H I fluctuations on sub-AU scales. B0329+54 has a parallactic distance of $1.03^{+0.13}_{-0.12}$ kpc and a proper motion of 95^{+12}_{-11} km s^{-1} (Brisken et al. 2002). The pulsar's proper motion corresponds to scales of 0.03 AU in one day and 1 AU in one month for an H I cloud halfway to the pulsar.

2. OBSERVATIONS

The 100 m GBT of the National Radio Astronomy Observatory (NRAO)[4] was used for this measurement. The GBT is an unblocked aperture telescope with a spatial resolution of 9″.2 at 21 cm. The system temperature on cold sky was ∼20 K. The detector was the NRAO spectral processor, a fast Fourier transform (FFT) spectrometer, configured to have 1024 channels for each linear polarization with a bandwidth of 1.25 MHz, producing a spectral resolution of 0.26 km s^{-1} per channel. The accumulation memory is 32-bit, providing good dynamic range. The spectral processor integration time was 14 pulse periods, approximately 10 s.

The pulsar B0329+54 is an ideal target for study of small-scale structure in cold H I. It is very bright, so a change in

---

[1] National Radio Astronomy Observatory, P.O. Box 2, Green Bank, WV 24944.

[2] Department of Physics and Astronomy, Colgate University, Hamilton, NY 13346.

[3] Current address: University of Hawaii, Honolulu, HI 96822.

opacity of 0.1 can be detected in a time less than the scintil-
lation timescale of ∼15 minutes. Its declination is such that
it can be observed by the GBT continuously for ∼20 hr dur-
ing which ∼50 scintles are seen. The observations reported
here were made in 18 separate observing sessions. Three long
(∼20 hr) sessions, separated by 2 weeks, were made to probe
H I fluctuations on sub-AU scales. Fifteen short (∼1−2 hr) ob-
servations spread over the subsequent 15 months sample scales
larger than an AU.

The data were calibrated using a method similar to that de-
scribed by Weisberg (1978). For each integration an absorption
spectrum was formed by taking the difference between the pul-
sar "on" and pulsar "off" spectra. If $\tau_{i,j}$ is the H I opacity for the
ith spectral channel and the jth integration sample, then

$$T_{i,j}(p_{\rm on})e^{-\tau_{i,j}} = \frac{T_{i,j}(p_{\rm on},l_{\rm on}) - T_{i,j}(p_{\rm off},l_{\rm on})}{T_{i,j}(p_{\rm off},l_{\rm off})\Big/ \sum_{i=1}^{n_{\rm chan}} T_{i,j}(p_{\rm off},l_{\rm off})}, \quad (1)$$

where $n_{\rm chan}$ is the number of spectral channels; T denotes in-
tensity in units of kelvins, where, for example, $T_{i,j}(p_{\rm off},l_{\rm on})$
corresponds to the intensity at the frequency of the H I line
emission when the pulsar is off and $T_{i,j}(p_{\rm on})$ corresponds to the
intensity at all observed frequencies when the pulsar is on. The
power is converted from detector counts to kelvins by using a
calibrated noise diode that was injected into every pulsar cycle
for 10% of the pulsar period. Each integration is then weighted
and summed such that

$$\langle T_i(p_{\rm on})\rangle e^{-\tau_i} = \frac{\sum_{j=1}^{n_{\rm int}} T_{i,j}(p_{\rm on})e^{-\tau_{i,j}}\left[T_{i,j}^2(p_{\rm on},l_{\rm off})/T_{{\rm sys}_{i,j}}^2\right]}{\sum_{j=1}^{n_{\rm int}}\left[T_{i,j}^2(p_{\rm on},l_{\rm off})/T_{{\rm sys}_{i,j}}^2\right]}, \quad (2)$$

where $T_{{\rm sys}_{i,j}}$ is the system temperature, $\langle T_i(p_{\rm on})\rangle$ is the weighted
average pulsar flux, and there are $n_{\rm int}$ independent integration
samples.

The flux from B0329+54 varies for two reasons: (1) pulse-to-
pulse variations due to intrinsic emission variations and (2) due
to scintillation. Because B0329+54 varies in intensity during
our 10 s integration period and can be a significant fraction of
the total system temperature, some of the emission spectrum
will appear in the absorption spectrum as "ghosts." Weisberg
(1978) has shown that the measured pulsar absorption spec-
trum is a linear combination of $T_i(p_{\rm off},l_{\rm on})$ and the desired pul-
sar absorption spectrum. Therefore, the measured H I emission
spectrum is used to fit and remove the observed ghosts. Simul-
taneously, a polynomial model is used to remove the average
pulsar flux ($\langle T_i(p_{\rm on})\rangle$), which cannot be independently measured,
and any structure in the baseline due to instrumental effects. The
ghost and polynomial fit is constrained only in spectral regions
where there is no H I absorption. The ghost spectrum and the
polynomial fit is then extrapolated through the regions with H I
absorption. Since the 1.25 MHz bandwidth of these observa-
tions is a significant fraction of the scintillation bandwidth[5] for
B0329+54 (measured to be 5.1 ± 0.1 MHz at 1640 MHz by
Minter 2001), the average pulsar flux contains scintillation-
induced structures that vary slowly with frequency. In order to
remove the baseline structure arising from scintillation struc-
tures and instrumental effects, a fifth-order polynomial is used.

---

[5] The scintillation bandwidth is the e^{-1} scale over which the pulsar's signal
becomes decorrelated in frequency due to scintillation of the pulsar signal from
a nonuniform distribution of electrons in the ISM. It effectively represents the
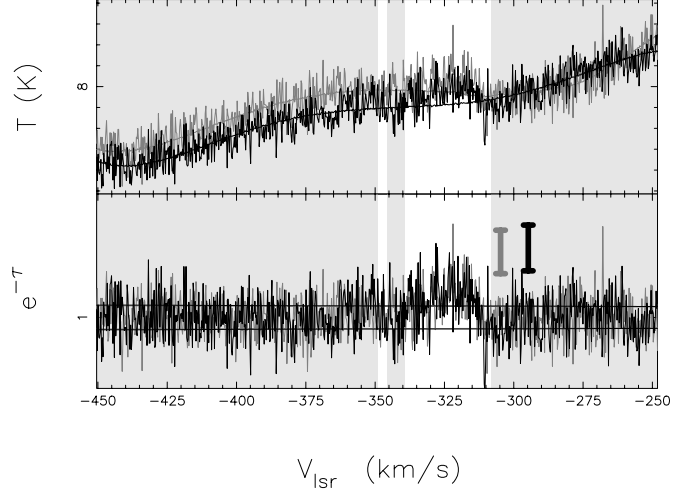average frequency domain size of an observed scintle.

FIG. 1.—*Top*: Spectrum of $\langle T_i(p_{\rm on})\rangle e^{-\tau_i}$ for two polarizations (X and Y)
toward 0329+54 and offset in frequency from the H I line. The smooth, solid
curves are the polynomial fits to the data. The gray area denotes the channels
used in the polynomial fit, whereas the white area is where the polynomial was
extrapolated. The same regions (by channel number) used here were also used
for the H I line data. *Bottom*: Resulting spectrum of $e^{-\tau_i}$. The straight lines
indicate the 1 σ level of the random noise, and the thick error bars indicate the
1 σ errors in extrapolating the polynomial.

For each integration the rms noise was computed for the
part of the spectrum without H I line emission for both $T_j(p_{\rm on})$
and $T_j(p_{\rm off})$. Since the H I line emission contributes signifi-
cantly to the system temperature (∼20 K), the rms noise will
be larger for frequencies where there is H I line emission. Thus,
the frequency-dependent noise is given by

$$\sigma_{T_{i,j}(p_{\rm on})} = \sigma_{T_j(p_{\rm on})}\left(1 + T_i^{\rm H I}\Big/T_{\rm sys}\right), \quad (3)$$

where $T_i^{\rm H I}$ is the H I line emission strength in the ith spectral
channel. A similar expression is used for $\sigma_{T_{i,j}(p_{\rm off})}$. These errors
are then propagated for all subsequent calculations.

Systematic errors are also important in the comparison of H I
absorption toward pulsars from different epochs. The system-
atic errors arise from the removal of the average pulsar flux,
$\langle T_i(p_{\rm on})\rangle$, via a polynomial fit from the results of equation (2) in
order to determine the $e^{-\tau}$ spectra. The actual pulsar flux will
certainly not follow the value of the polynomial, as it is extrap-
olated over the regions of H I absorption that were excluded
from the polynomial fitting. This difference between the ac-
tual pulsar flux and the extrapolated polynomial value results in
a systematic error that must be taken into account when com-
paring the H I absorption spectra between different epochs.

In Figure 1 we show an example of how the systematic error
is calculated. A frequency band without H I emission or ab-
sorption was observed and reduced in the same manner as the
pulsar H I absorption data. The top panel of Figure 1 shows the
results of equation (2) and the polynomial fit. The polynomial
fit has only been done in the shaded regions, which are the same
channel numbers used for the polynomial fit for the H I ab-
sorption measurements. The bottom panel of Figure 1 shows
the resulting $e^{-\tau}$ spectrum. As can been seen in Figure 1, there
is excess noise in the regions where the polynomial fit was
extrapolated (the white areas in Fig. 1). This systematic noise
is shown by the single error bar above the data in the bottom
panel of Figure 1. The random noise is shown by the two solid
lines in the bottom panel of Figure 1. The systematic noise
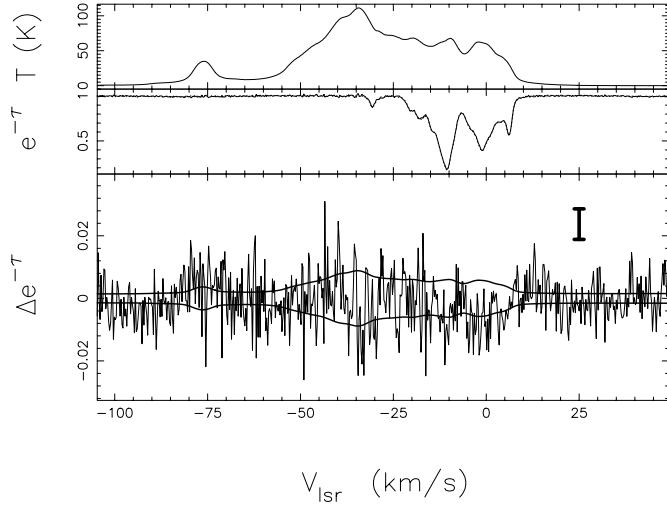was determined by (1) subtracting the polynomial obtained by

Fig. 2.—*Top*: H I emission spectrum toward B0329+54. *Middle*: Absorption spectra from 2002 July 14 (*solid line*) and 2003 July 2 (*dotted line*). *Bottom*: Difference between the two absorption spectra. The lines above and below the spectrum are the 1 σ uncertainties. The uncertainty is a function of frequency, since the H I emission contributes significantly to the total system temperature. The 1 σ uncertainty in extrapolating the polynomial fit to the pulsar emission spectrum across the H I line is shown by the individual error bar.

omitting the H I absorption channels (shown in Fig. 1) with a polynomial obtained by using all of the channels and (2) taking the rms of the difference between these two fitted spectra over the omitted channel ranges.

The average systematic error found using this method amounts to ±0.005 in the $e^{-\tau}$ spectra. Given that previous detections of H I fluctuations have been recently questioned (e.g., Johnston et al. 2003; Stanimirović et al. 2003), we choose to be conservative in our error estimates. The quoted uncertainties for our measurements thus contain both random and systematic errors, which have been added in quadrature. We use a value of ±0.005 in the $e^{-\tau}$ spectra, as determined above, for the systematic errors in all H I spectra.

3. RESULTS

Figure 2 compares the absorption spectrum toward B0329+54 for two epochs, 2002 July 14 and 2003 July 2. The solid lines

above and below the difference spectrum are the 1 σ random noise uncertainties. The systematic error from the polynomial fitting is indicated by the error bar above the data. There are no significant differences between the two spectra shown in Figure 2. In fact, no variations have been detected over the entire 16 months of observations.

The structure function for time variations in the opacity is defined as

$$D_\tau(\Delta t, i) = \langle [\tau(t, i) - \tau(t + \Delta t, i)]^2 \rangle, \qquad (4)$$

where $\tau(t, i)$ is the opacity at time t in the ith spectral channel. The structure function is actually computed by binning values of $[\tau(t, i) - \tau(t + \Delta t, i)]^2$ and then averaging the data within a given bin. The errors for the structure function are computed from the distribution of values within a given bin. Analysis of the data using a structure function has two advantages: (1) it reduces the noise for a given delay through averaging, and (2) it provides information on the power spectrum of H I absorption fluctuations. If the power spectrum of opacity variations is a power law, as is the case for turbulent fluctuations, then the structure function will also be a power law. If only noise is present in the data, then the structure function will be constant at a level of $2\sigma_{\tau(i)}^2$. (We refer the reader to Spangler et al. [1989] for a more detailed discussion of structure functions.)

Figure 3 plots the structure function for our observations of B0329+54 for two frequency channels. The structure function data are consistent with there being no turbulence in the H I absorption down to our detection limits. Figure 4 shows our observational upper limits to the turbulent fluctuations in opacity derived from the structure functions in each spectral channel. The data cover differences between 10 minutes and 16 months corresponding to angular scales of 0.37 μas to 23.8 mas and geometric linear size scales of 0.0025–12.5 AU, assuming H I gas halfway to the pulsar and using the pulsar's proper-motion velocity of 95 km s^{-1} and distance of 1.03 kpc. (For the remainder of this paper we calculate distance scales assuming a distance halfway to the pulsar of 515 pc.) Furthermore, comparing our spectra to those of Gordon et al. (1969), who first detected H I absorption toward B0329+54, shows no evidence for variations in H I absorption greater than $\Delta e^{-\tau} \sim 0.01$ (the noise level of the Gordon et al. measurements is $\Delta e^{-\tau} \sim 0.01$,
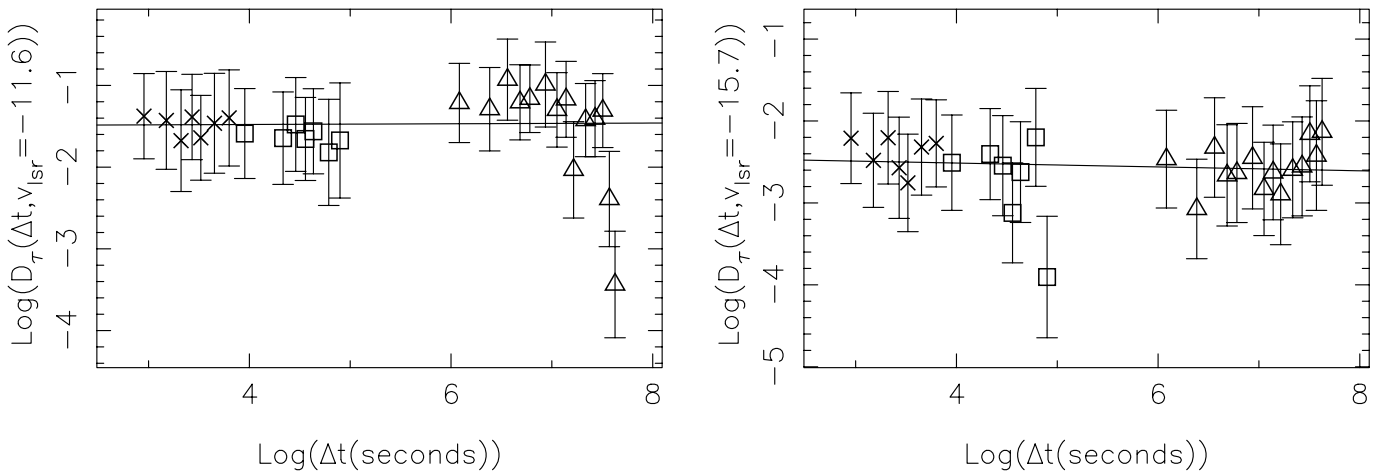

Fig. 3.—Structure function of τ for the spectral channels centered on $v_{\rm LSR} = -11.6$ km s^{-1} (*left*), at the peak of the absorption line, and $v_{\rm LSR} = -15.7$ km s^{-1} (*right*), halfway down the absorption line, with 3 σ error bars. The crosses are data averaged over a single scintle, the squares consist of ~2 hr averages within a given epoch, and the triangles are data averaged over a single observing epoch. The best-fit power laws are shown as the solid lines and are given by $(-1.5 \pm 0.1) + (0.00 \pm 0.02) \log(\Delta t)$ and $(-2.4 \pm 0.1) + (-0.02 \pm 0.02) \log(\Delta t)$, respectively. No turbulent H I opacity fluctuations are detected on any scale between 0.0025 and 12.5 AU.
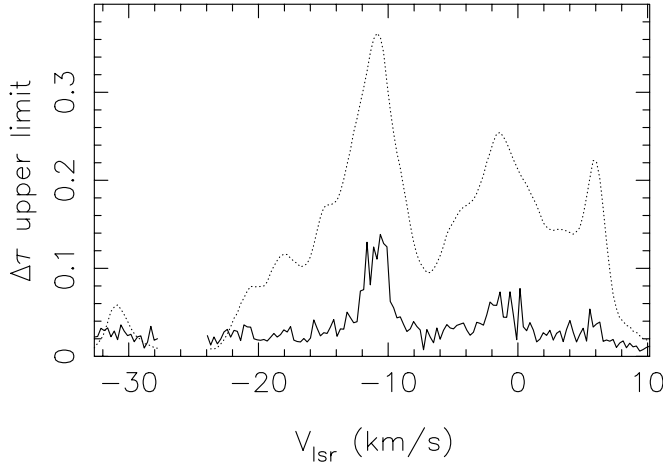
Fig. 4.—Upper limits to $\Delta\tau$ from our measurements (*solid line*) and from the scintillation model of Gwinn (2001; *dotted line*). The frequency dependence of the $\Delta\tau$ upper limits follows the expected noise contributions due to the change in system temperature from the H I emission and absorption.

Fig. 5.—Upper limits to the spin temperature, T_s, of the H I responsible for the absorption toward B0329+54.

while the noise for our measurements is $\Delta e^{-\tau} \sim 0.002$) with a velocity resolution of 1.7 km s^{-1}. This corresponds to a linear scale of $\sim$350 AU.

Strong interstellar scintillation is observed toward B0329+54. The multipath propagation that results from scintillation effectively creates a spatial smoothing of H I absorption structures within the observed angularly broadened size of the pulsar, which might mask absorption variations that exist on very small scales. Semenkov et al. (2003) have limited the angular broadening size of B0329+54 at 1600 MHz to be $\leq$1.8 mas, corresponding to a scintillation smoothing scale of $\leq$1.15 AU assuming a λ^2 scaling of the angular broadening size. Our observations probe scales up to 12.5 AU, and thus scintillation cannot account for a lack of H I absorption fluctuations in the data. The scintillation smoothing provides a lower limit to the smallest scale opacity structure that we can probe. However, we only have upper limits to the scattering disk size. Therefore, we use the geometric linear size scale of 0.0025 AU (see above) rather than the scattering disk size as the smallest size scale probed by our observations.

Gwinn (2001) suggests that interstellar scintillation coupled with gradients in the Doppler velocity of H I can produce small-scale fluctuations in H I absorption spectra toward pulsars. The GBT observations of B0329+54 can decouple density fluctuations from velocity gradients, since an absorption spectrum can be measured for individual scintles. The data points in Figure 3 are divided into three groups. The crosses are data averaged over a single scintle, the squares consist of $\sim$2 hr averages within a given epoch, and the triangles are data averaged over a single observing epoch. No turbulent fluctuations are detected on any timescales from the scintillation timescale to 16 months in our observations.

Gwinn (2001) predicts that the opacity variations that would be observed are given by $\sigma_\tau = (\tau\Delta v/c_s)^{1/2}$, where Δv is the amount by which the velocity of the absorption feature changes and c_s is the thermal sound speed. We have fitted Gaussians to the peak absorption features for each epoch. From these fits we find no trend in the value of the line center and can limit any change in velocity of the absorbing gas to $\Delta v < 0.065$ km s^{-1}. We can derive upper limits to the thermal sound speed from the H I spin temperature (T_s) found from comparing the H I emission spectrum (T_{em}) with the H I absorption spectrum. The spin
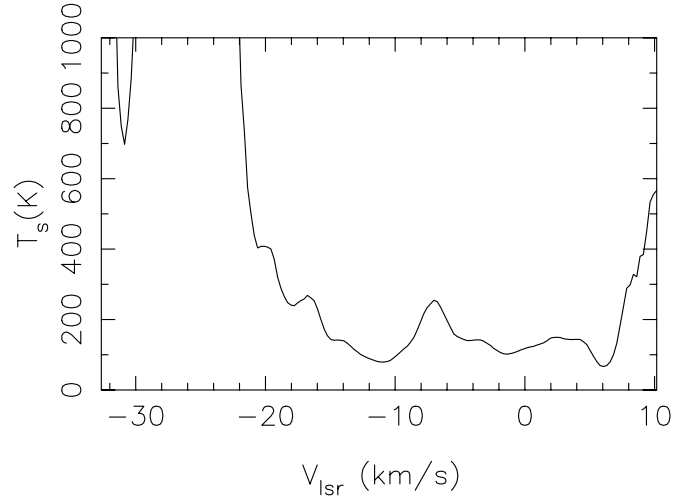
temperature is found from $T_s = T_{em}/1 - e^{-\tau}$ and should be considered an upper limit, since some warm H I contributes to T_{em} but typically does not contribute to the H I absorption. The spin temperature upper limits are shown in Figure 5. The sound speed can then be estimated from $c_s = 0.093[T_s(K)]^{1/2}$ km s^{-1}. An estimate of Gwinn's σ_τ prediction is shown as the dotted line in Figure 4. The derived spin temperatures are not likely to be incorrect by more than a factor of a few. We thus consider the predictions using Gwinn's formula for opacity variations shown in Figure 4 to be a reasonable upper limit for opacity variations induced by the combination of scintillation and velocity gradients. From Figure 4 it can be seen that our measured limits are smaller than the upper limits determined for Gwinn's σ_τ formula. Although this suggests that Gwinn's hypothesis could be incorrect, we cannot claim this with any certainty, since only an upper limit can be determined for Gwinn's prediction.

4. DISCUSSION

Our GBT observations toward B0329+54 were made primarily to probe sub-AU H I structures. The structure functions of the change in opacity versus time are consistent with noise (i.e., the structure functions are constant values). The structure functions thus place upper limits on the opacity variations, as discussed in § 3. So we do not detect H I opacity variations consistent with a turbulent power-law distribution on scales <12.5 AU greater than 0.026 for the -31, -21, -18, and $+4$ km s^{-1} absorption lines, 0.12 for the -11 km s^{-1} absorption line, and 0.055 for the -1 km s^{-1} absorption line. This is somewhat surprising, since Frail et al. (1994) detected H I variations of $\Delta\tau \sim 0.1$ in all observed pulsars. However, Johnston et al. (2003) have made multiepoch observations of H I absorption toward four southern pulsars and find no significant variations, and Stanimirović et al. (2003) reach a similar conclusion from reobservations of the Frail et al. pulsars to increase the number of temporal baselines. Very Long Baseline Array (VLBA) H I absorption measurements have been summarized by Faison (2002). Only two sources show significant H I fluctuations. Small-scale H I structure measured through H I absorption is currently found in only two of the 15 sources observed in Johnston et al. (2003), Stanimirović et al. (2003), Faison (2002), and this work.

On large scales the distribution of H I is influenced by spiral density waves, supernovae, etc., as is evident by the observed

shells and filaments in neutral hydrogen surveys. Dickey & Lockman (1990) have argued that no more than 10% of the total H I exists in small-scale structures ($\leq$1 pc). That is, there are not large variations in the H I column density on small spatial scales, and the concept of distinct H I clouds does not describe most of the Galactic neutral hydrogen. The distribution of H I can be analyzed by producing angular power spectra of H I emission over different spatial scales. The results are well fitted by a power law with a slope of approximately -3 toward different directions in the Galaxy (e.g., Crovisier & Dickey 1983; Green 1993; Dickey et al. 2001). These results can be described by a turbulent cascade of energies (Lazarian & Pogosyan 2000). But does this turbulence extend down to very small spatial scales? In other words, what is the inner scale of the turbulence?

We are unable to answer this question with the current data on B0329+54, since we have not detected any significant turbulent H I fluctuations.

Of particular note are the results of Shishov et al. (2003) from diffractive scintillation measurements of B0329+54. They find that on scales below 3×10^{16} cm the diffractive scintillation can be explained with a scattering screen comprised solely of ion- ized gas.[6] However, on scales above 3×10^{16} cm their results require that some neutral gas is also present within the scattering screen. Could this indicate that the inner scale for the neutral gas is 2000 AU? If this is the inner scale, then an H I density of 1 cm^{-3} at a temperature of 100 K would give a kinematic viscosity of 3×10^{21} cm^2 s^{-1}.

---

[6] The value 3×10^{16} cm was obtained by Shishov et al. (2003) using a velocity of 139 km s^{-1} for the pulsar. Using a velocity of 95 km s^{-1}, as measured by Brisken et al. (2002), results in a scale of 2×10^{16} cm.

REFERENCES

Brisken, W. F., Benson, J. M., Goss, W. M., & Thorsett, S. E. 2002, ApJ, 571, 906
Crovisier, J., & Dickey, J. M. 1983, A&A, 122, 282
Deshpande, A. A. 2000, MNRAS, 317, 199
Dickey, J. M., & Lockman, F. J. 1990, ARA&A, 28, 215
Dickey, J. M., McClure-Griffiths, N. M., Stanimirović, S., Gaensler, B. M., & Green, A. J. 2001, ApJ, 561, 264
Faison, M. D. 2002, in ASP Conf. Ser. 276, Seeing Through the Dust, ed. A. R. Taylor, T. L. Landecker, & A. G. Willis (San Francisco: ASP), 324
Frail, D. A., Weisberg, J. M., Cordes, J. M., & Mathers, C. 1994, ApJ, 436, 144
Frisch, U. 1995, Turbulence: The Legacy of A. N. Kolmagorov (Cambridge: Cambridge Univ. Press)
Gordon, C. P., Gordon, K. J., & Shalloway, A. M. 1969, Nature, 222, 129
Green, D. A. 1993, MNRAS, 262, 327
Gwinn, C. R. 2001, ApJ, 561, 815
Heiles, C. 1997, ApJ, 481, 193
Johnston, S., Koribalski, B., Wilson, W., & Walker, M. 2003, MNRAS, 341, 941
Lazarian, A., & Pogosyan, D. 2000, ApJ, 537, 720
Minter, A. 2001, Ap&SS, 278, 159
Semenkov, K. V., Popov, M. V., Soglasnov, V. A., & Hirabayashi, H. 2003, Astron. Lett., 29, 96
Shishov, V. I., et al. 2003, A&A, 404, 557
Spangler, S. R., Fanti, R., Gregorini, L., & Padrielli, L. 1989, A&A, 209, 315
Stanimirović, S., Weisberg, J. M., Hedden, A., Devine, K., & Green, T. 2003, ApJ, 598, L23
Tennekes, H., & Lumley, J. L. 1994, A First Course in Turbulence (Cambridge: MIT Press)
Weisberg, J. M. 1978, Ph.D. thesis, Univ. Iowa